Supplementary information for "Confronting the water potential information gap"

Section S1 – Water retention curves (Main Text Figure 2a-d): The water retention curves in Figure 2 of the main text were created using the van Genuchten model (van Genuchten 1980) relating soil water potential (Ψ_S) to soil moisture content (θ):

$$\Psi_S = \frac{\left(\Theta^{-1/m} - 1\right)^{1/n}}{\alpha} \qquad [S1]$$

where *n* and *m* are dimensionless shape parameters related by

$$m = 1 - 1/n. \qquad [S2]$$

The α is a parameter linked to the inverse of the air entry values (cm^{-1}), and Θ is relative soil moisture defined as:

$$\Theta = \frac{\theta - \theta_r}{\theta_s - \theta_r}, \qquad [S3]$$

where θ_r is the residual water content (cm^3 cm^{-3}) and θ_s is the saturated water content (cm^3 cm^{-3}). For each soil type, the α, θ_r, and θ_S were selected as the mean values reported in the updated ROSETTA pedo-transfer function (Zhang & Schaap 2017, see Supplementary Table S1). The *n* was allowed to vary by randomly selecting a value from a uniform distribution bounded by ± 1 standard deviation (as reported by Zhang & Schaap) from the mean for each soil type, resulting in the ranges shown in Table S1. The *m* was determined for each randomly chosen *n* through Eq. S2. A total of 100 curves were generated this way, and the uncertainty illustrated in Figure 2 represents the 90% confidence interval around Ψ_s at a given θ.

Supplementary Table S1*: The van Genuchten parameter values or ranges used to parameterize the water retention curves in Figure 2 of the main text, from Zhang & Schaap (2017) and available from http://www.u.arizona.edu/~ygzhang/download.html. The parameter 'm' was derived from 'n' using Eq. S2.*

	α	θ_r	θ_s	n
Loamy Sand	0.0246	0.058	0.383	1.45 – 1.97
Silt	0.00604	0.065	0.47	1.40 – 1.78
Silty Clay	0.0101	0.117	0.124	1.16 – 1.40

Section S2: The HYDRUS simulations (Main text Figure 2e-g): Variability in the water retention curve linked to pedo-transfer uncertainty was then propagated into predictions of Ψ_S and θ (at depths of 15 cm) and surface evapotranspiration (ET, cm day) using the HYDRUS 1D soil water dynamics model (Simunek et al. 2005). Fifty simulations were performed for the Bradford Woods deciduous forest site in south-central Indiana, where the HYDRUS 1D model had been previously calibrated as described in Naylor et al. (2016). In general, model settings were left unchanged, with a few exceptions. First, rooting depth was constrained to a constant 100 cm, and the leaf area index (LAI) was constrained to a constant value of 5 m^3/m^3. These estimates of root depth and LAI were informed by observations from the nearby Morgan-Monroe State Forest deciduous forest site (Roman et al. 2015), where ground-based LAI observations have been collected since 1998, and root depth was recently estimated from soil pits dug at two locations at the site. In Morgan-Monroe, while some tap roots may extend to the bedrock (typically between 1-2 m deep), the majority of roots were constrained to the upper 100 cm of the soil. Finally, the parameters of the water stress reduction function were adjusted (specifically, P_o = -10 cm, $P_{o,pt}$ = -25 cm, P2H and P2L = -1000 cm, and P3 = -55000 cm) to allow evapotranspiration to remain positive during most of the 2012 drought event, informed by direct observations of ET from Morgan-Monroe (Roman et al. 2015, Sulman et al. 2016) during the same drought. In Morgan-Monroe, ET was decreased by the drought, but never reached zero.

The soil at Bradford Woods is characterized by a 40 cm depth AP horizon dominated by sandy loam, and a BW Horizon dominated by silt loam from a depth of 40 cm to 208 cm (Naylor et al. 2016). The very bottom of the soil layer (depths 208 – 230 cm) was prescribed to be clay loam. The parameters of the van Genuchten model used in the HYDRUS simulations are shown in Table S2, where again most were held constant, but *n* and *m* varied for the sandy and silt loam layers by drawing *n* from within one standard deviation of its distribution as reported by Zhang & Schaap (2017). The shaded areas in Figure 2e-g thus illustrate the resulting variation in ET, θ, and Ψ_S due solely to variability in *n* and *m.*

Table S2 *The van Genuchten parameter values or ranges used in the simulations described in Figure 2e-g. The parameter 'm' was derived from 'n' according to Equation S2.*

	Depth	α	θ_r	θ_s	n
Sandy loam	0 – 40 cm	0.0016	0.061	0.381	1.29 – 1.66
Silt loam	40 – 208 cm	0.0034	0.083	0.427	1.35 - 1.79
Clay loam	208 – 230 cm	0.0099	0.107	0.429	1.23

Section S2: The ORCHIDEE Model Simulations (main text Figure 3): The ORCHIDEE land surface model is the terrestrial part of the IPSL (Institute Pierre-Simon Laplace) Earth system model (Boucher et al. 2020, Lurton et al. 2020). In this study, the CMIP6 version of this model is used. As a complex land surface model, ORCHIDEE models the water, energy, and carbon cycles to simulate the interactions between the biosphere and atmosphere. The hydrology model in ORCHIDEE discretizes the first 2 m of the soil column over 11 layers which is used to solve the Richards diffusion equation. Hydraulic conductivity and diffusivity needed to solve this equation, as well as Ψ_S, are calculated in ORCHIDEE using the van Genuchten model described above (Eq S1-S3). For this experiment, we ran ORCHIDEE over three single mesh locations using local half-hourly forcing data to drive the model at each site (see Table S3), and used GPP modeled at a daily time-step.

ORCHIDEE has a lot of internal parameters linked to many different processes (e.g. see Table S4). It is important to understand which outputs are sensitive to which parameters, especially when developing the model and improving through data assimilation experiments. As such, it is common practice to perform a sensitivity analysis of the parameters. To help sample parameter space and execute the SA algorithms in this study, we used the SALib python package (Herman and Usher 2017).

The sensitivity analysis results shown in the main text are generated using Sobol's method (Sobol 2001). However, this method needs lot of model simulations for it to be effective, and the number of simulations required scales with the number of parameters. As such, it was crucial to minimize the number of parameters tested. This was done in two steps. Firstly, two scaling factors were added to the code to control some of the model processes (namely soil thermal conductivity and heat capacity). These were used to avoid adding all the parameters controlling these processes in the sensitivity analysis. If the model outputs tested had been found to be sensitive to these scaling factors, then the internal parameters would have been considered. Fortunately, they were not.

Secondly, the parameters were filtered using a Morris sensitivity analysis (Morris 1991; Campolongo et al. 2007). Since the Morris algorithm only requires a relatively low number of simulations to highlight sensitive parameters, it is a useful algorithm to use as a first step. Results from this second step can be found in Raoult et al. 2021 for a similar experiment. Through the Morris experiment, we reduced the number of parameters (and scaling factors), from 38 to 29 parameters by removing all parameters that did not influence GPP. Using these remaining 29 parameters, a total of 60,000 simulations were performed for each site before calculating the Sobol Indices.

Both sensitivity analysis algorithms (Morris and Sobol) test the sensitivity of scalar model outputs to the parameters. Therefore, to test the sensitivity of modelled daily GPP values, and to retain all the information from the full timeseries, model-data RMSE (root-mean squared error) was used. The FLUXNET2015 database (Pastorello et al., 2020) was used to provide both the observations and the driving data for the sites tested. FLUXNET2015 contains flux data from a number of different networks around the globe, allowing us to test three sites in very diverse climates. FLUXNET2015 data are processed in a manner similar to the algorithms implemented in ReddyProc (Pastorello et al. 2020). The night-time partitioning algorithm (Reichstein et al. 2005) was selected for the GPP estimates.

Ranges over which the parameters were allowed to vary during the experiment were either chosen from literature/expert knowledge, or, when no such data were unavailable, chosen as +/- 20% from their default value i.e., the value used in ORCHIDEE when performing a standard simulation. We also ensured that relationship between parameters were maintained where such restriction existed (e.g., $\theta_r < \theta_s$).

Finally, Figure 3 in the manuscript shows the total contribution of each parameter, including both the independent contributions and the interactions.. The individual effect of each parameter can be seen below in Figure S1. When considering only the independent effects, the water retention curve parameters explain: 9.9% of the variance over the TeBF, 7.4% of variance over the BoNF and 59.1% of the variance over SaS. For the wider set of soil hydrology parameters, this increases to 19.6%, 16.9% and 79.1% for TeBF, BoNF and SaS, respectively. The individual contribution of each parameter is therefore still significant, especially in the semi-arid site.

Table S3: FLUXNET2015 sites for Figure 3. MAT and MAP are mean annual temperature (°C) and mean annual precipitation (mm/year), respectively.

Site Name	Site ID	Lat	Lon	MAT, MAP	Biome	Reference
Harvard Forest ESM tower (United States)	US-Ha1	42.538	72.172	6.62, 1071	Deciduous Broadleaf Forests (TeBF)	Urbanski et al. 2007
Sodankyla (Finland)	FI-Sod	67.362	26.639	-1, 500	Evergreen Needleleaf Forests (BoNF)	Thum et al. 2007
Demokeya (Sudan)	SD-Dem	13.283	30.478	26, 320	Semi-Arid Savanna (SaS)	Ardö et al. 2008

Table S4: ORCHIDEE parameters used for Figure 3. The default values are shown, followed in brackets by the ranges over which they were allowed to vary for each site tested. Further details about each parameter can be found in Raoult at al. 2021.

Parameter	Description	TeBF Soil: Sandy loam	BoNF Soil: Loam	SaS Soil: Sandy loam
n	van Genuchten water retention curve coefficients (-/mm^{-1})	1.89 [1.09, 2.69]	1.56 [1.10, 2.20]	1.89 [1.09, 2.69]
α		0.0075 [0.0045, 0.0105]	0.0036 [0.002,0.0050]	0.0075 [0.0045, 0.0105]
θ_r	Residual volumetric water content	0.065 [0.039, 0.078]	0.078 [0.047, 0.0936]	0.065 [0.039, 0.078]
θ_s	Saturated volumetric water content (m^3.m^{-3})	0.41 [0.37, 0.57]	0.43 [0.37, 0.57]	0.41 [0.37, 0.57]
K_s	Hydraulic conductivity at saturation (mm.d^{-1})	1060.8 [636.5, 1485.1]	249.6 [149.8, 349.4]	62.4 [37.4, 87.4]
θ_f	Volumetric water content at field capacity (m^3.m^{-3})	0.32 [0.19, 0.37]	0.32 [0.19, 0.37]	0.32 [0.19, 0.37]
θ_w	Volumetric water content at wilting point (m^3.m^{-3})	0.1 [0.08, 0.18]	0.1 [0.10, 0.18]	0.1 [0.08, 0.18]
%p	Percentage of soil moisture above which transpiration is maximal	0.8 [0.3, 1]	0.8 [0.3, 1]	0.8 [0.3, 1]
$root_{profile}$	Root profile (m^{-1})	0.8 [0.2, 3]	1 [0.25, 4]	1 [0.25, 4]
$evap_{resistance}$	Factor controlling bare soil resistance to evaporation	1 [0, 1.2]	1 [0, 1.2]	1 [0, 1.2]
C	Parameter controlling shape of waterstress curve	1 [0.05, 10]	1 [0.05, 10]	1 [0.05, 10]
VC_{max}	Maximum carboxylation rate (µ.molm^{-2}.s^{-1})	55 [30, 80]	35 [19, 51]	70 [38, 102]
b1	Empirical factor involved in calculating the leaf-to-air vapor pressure difference	0.14 [0.05, 0.2]	0.14 [0.05, 0.2]	0.14 [0.05, 0.2]
LAI_{max}	Maximum lead area index (m^2.m^{-2})	4.5 [3.0, 8.0]	4.0 [3.0, 8.0]	2.0 [1.0, 3.5]
Lagecrit	Critical leaf age (days)	180 [120, 240]	910 [610, 1210]	120 [30, 180]
SLA	Specific leaf area (m^2.g^{-1})	0.026 [0.013, 0.05]	0.00926 [0.004, 0.02]	0.026 [0.013, 0.05]

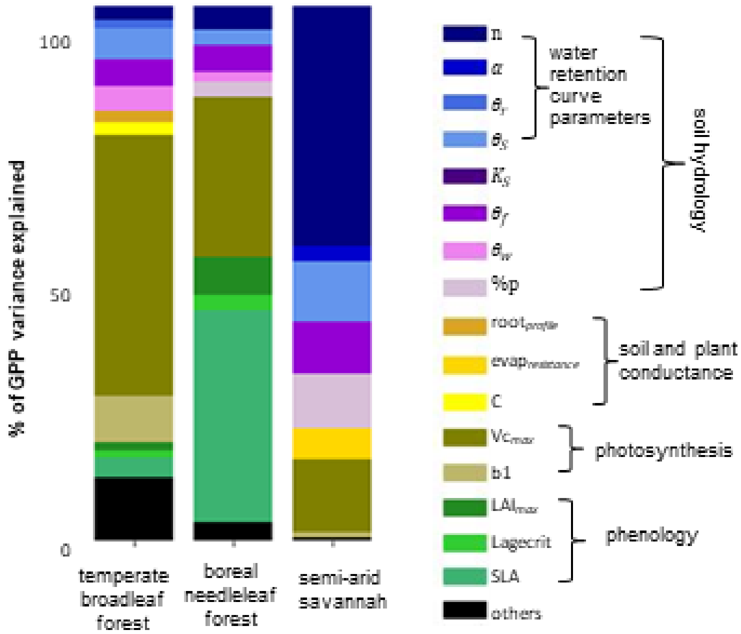

Figure S1: Same as Figure 4 in the main text, but showing only independent contributions of each model parameter for explaining GPP.

<u>Section S4: The AmeriFlux GPP analysis (main text Figure 4):</u>

Table S5 provides details on the AmeriFlux sites used in the analysis informing Figure 4 of the main text. Data from these flux towers was acquired from the AmeriFlux network (ameriflux.lbl.gov) and subjected to a standardized quality control, gapfilling, and partitioning approach using the ReddyProc software (Wutzler et al. 2018). We used the "nighttime" partitioning approach (Reichstein et al. 2005) for estimating gross primary productivity (GPP) from the measured net ecosystem exchange.

Table S5: AmeriFlux sites for Figure 5. MAT and MAP are mean annual temperature (ºC) and mean annual precipitation (mm/year), respectively.

Site Name	Site ID	Lat	Lon	MAT, MAP	Biome	Reference
Morgan-Monroe State Forest	US-MMS	39.323	-86.413	10.9, 1032	Deciduous Broadleaf forest	Roman et al. 2015
Santa Rita Mesquite	US-SRM	31.821	-110.866	17.9, 380	Woody Savanna	Scott et al. 2009
Tonzi Ranch	US-TON	38.431	-120.966	15.8, 559	Woody Savanna	Ma et al. 2012
Missouri Ozarks	US-MOz	38.744	-92.200	12.11, 986	Deciduous Broadleaf Forest	Gu et al. 2016

References cited in this document:

Ardö, J., Mölder, M., El-Tahir, B.A. and Elkhidir, H.A.M.: Seasonal variation of carbon fluxes in a sparse savanna in semi arid Sudan, *Carbon Balance and Management* **3,** 1-18. (2008).

Boucher, O. *et al.* Presentation and evaluation of the IPSL-CM6A-LR climate model. *Journal of Advances in Modeling Earth Systems* **12**, e2019MS002010 (2020).

Campolongo, F., Cariboni, J., & Saltelli, A. An effective screening design for sensitivity analysis of large models. *Environmental Modelling & Software* **22**, 1509-1518. (2007).

Herman, J. and Usher, W. SALib: An open-source Python library for sensitivity analysis. Journal of Open Source Software **2**. doi:10.21105/joss.00097. (2017)

Lurton, T. *et al.* Implementation of the CMIP6 Forcing Data in the IPSL-CM6A-LR Model. *Journal of Advances in Modeling Earth Systems* **12**, e2019MS001940 (2020).

Morris, M. D. Factorial sampling plans for preliminary computational experiments. *Technometrics* **33**, 161-174. (1991)

Naylor, S., Letsinger, S.L., Ficklin, D.L., Ellett, K.M. and Olyphant, G.A.. A hydropedological approach to quantifying groundwater recharge in various glacial settings of the mid-continental USA. *Hydrological Processes* **30,** 1594-1608. (2016)

Pastorello, G., Trotta, C., Canfora, E. *et al.* The FLUXNET2015 dataset and the ONEFlux processing pipeline for eddy covariance data. *Scientific Data* **7,** 225 (2020).

Raoult, N., Ottlé, C., Peylin, P., Bastrikov, V., & Maugis, P. (2021). Evaluating and Optimising Surface Soil Moisture drydowns in the ORCHIDEE land surface model at in situ locations, *Journal of Hydrometeorology, in press. https://doi.org/10.1175/JHM-D-20-0115.1*

Reichstein, M., *et al.* On the separation of net ecosystem exchange into assimilation and ecosystem respiration: review and improved algorithm. *Global Change Biology* **11,** 1424-1439. (2005).

Roman, D.T., *et al*.. The role of isohydric and anisohydric species in determining ecosystem-scale response to severe drought. *Oecologia* **179,** 641-654 (2015).

Simunek, J., Van Genuchten, M. T. & Sejna, M. The HYDRUS-1D software package for simulating the one-dimensional movement of water, heat, and multiple solutes in variably-saturated media. *University of California-Riverside Research Reports* **3**, 1-240 (2005).

Sulman, B.N., Roman, D.T., Scanlon, T.M., Wang, L. and Novick, K.A. Comparing methods for partitioning a decade of carbon dioxide and water vapor fluxes in a temperate forest. *Agricultural and Forest Meteorology* **226,** 229-245. (2016).

Sobol, I. M. Global sensitivity indices for nonlinear mathematical models and their Monte Carlo estimates. *Mathematics and Computers in Simulation* **55,** 271-280. (2001)

Thum, T., Aalto, T., Laurila, T., Aurela, M., Kolari, P. and Hari, P.: Parametrization of two photosynthesis models at the canopy scale in a northern boreal Scots pine forest. *Tellus B: Chemical and Physical Meteorology* **59**, 874–890. (2007).

Urbanski, S. *et al.* Factors controlling CO2 exchange on timescales from hourly to decadal at Harvard Forest. *Journal of Geophysical Research: Biogeosciences* **112** (2007).

van Genuchten, M. T. A closed-form equation for predicting the hydraulic conductivity of unsaturated soils. *Soil Science Society of America Journal* **44**, 892-898 (1980).

Wutzler, T., *et al*. Basic and extensible post-processing of eddy covariance flux data with REddyProc. *Biogeosciences* **16,** 5015-5030 (2018).

Zhang, Y. & Schaap, M. G. Weighted recalibration of the Rosetta pedotransfer model with improved estimates of hydraulic parameter distributions and summary statistics (Rosetta3). *Journal of Hydrology* **547**, 39-53 (2017).